

# Effect of Lattice Strain on the Debye-Waller Factor of CuInSe<sub>2</sub> Nanoparticles

E. Purushotham

Department of Physics, SR Engineering College (Autonomous), Warangal, India

**Email address:**

psm45456@gmail.com

**To cite this article:**

E. Purushotham. Effect of Lattice Strain on the Debye-Waller Factor of CuInSe<sub>2</sub> Nanoparticles. *American Journal of Materials Synthesis and Processing*. Vol. 1, No. 4, 2016, pp. 43-46. doi: 10.11648/j.ajmsp.20160104.12

**Received:** September 6, 2016; **Accepted:** November 24, 2016; **Published:** January 9, 2017

**Abstract:** CuInSe<sub>2</sub> synthesized by a modified solvothermal route could be altered considerably by controlling the reaction temperature, reaction time and washing agents. Synthesized CuInSe<sub>2</sub> powders were characterized by X-ray diffraction. The particle size ( $t$ ), lattice strain ( $\epsilon$ ) and Debye-Waller factor ( $B$ ) were determined from the half-widths and integrated intensities of the Bragg reflections. The particle shape was spherical when demonized water was used as washing agent. Particles with the size down to 25.8nm were obtained. The variation of energy of vacancy formation as a function of lattice strain has been studied.

**Keywords:** X-ray Diffraction, Particle Size, Lattice Strain, Debye-Waller Factor, Vacancy Formation Energy

## 1. Introduction

CdSe in the form of nanorod had been developed as next generation cells emphasizing the low cost production [1–3]. CuInSe<sub>2</sub> is an I–III–VI<sub>2</sub> compound semiconductor with superior properties for photovoltaic applications [4]. The Debye-Waller factor is an important lattice dynamical property. But it is interesting to study the effect of particle size and lattice strains on the Debye-Waller factors of CuInSe<sub>2</sub>. There is considerable X-ray work on the Debye-Waller factors of CuInSe<sub>2</sub> particles can be synthesized by a solvothermal route [5, 6]. In this work, we adopt the same chemical method and successfully modified it to prepare the CuInSe<sub>2</sub> nano-rods. Crystalline phase and microstructure of CuInSe<sub>2</sub> nano-particles were characterized and reported in this article.

## 2. Experimental

CuInSe<sub>2</sub> particles were synthesized by a modified solvothermal route using a mixture of Se powder (2.59 mmol, 99.9% purity), CuCl<sub>2</sub> · 2H<sub>2</sub>O (1.26 mmol) and InCl<sub>3</sub> · 4H<sub>2</sub>O (1.29 mmol). The reagents were loaded into a 60 ml Teflon beaker and filled with anhydrous ethylenediamine as chelating agent up to 80% of the total volume. Chemical solution was stirred by a magnetic bar for 2 h. After mixing

thoroughly, the Teflon beaker was then sealed in a stainless steel container and heated in an oven by fixing the reaction temperature 200°C and the time varied from 10 to 20 hours. It was subsequently cooled to room temperature, the precipitate was then filtered and washed with absolute ethanol and distilled water several times in order to remove by-products. Finally, CuInSe<sub>2</sub> powders in black color were obtained after drying in an oven at 60°C for 3 h. We also used diethylamine as chelating agent in our experiments. Unfortunately, it caused the formation of second phases such as InSe and In<sub>2</sub>Se<sub>3</sub> in the final product. Thus, we normally use anhydrous ethylenediamine due to its capability to produce single-phase CuInSe<sub>2</sub> with higher purity and smaller particle size. The samples were then characterized by the following techniques:

(1) X-ray diffractometer (XRD): X-ray diffractograms were obtained with a Philips CWU 3710 X-ray powder diffractometer in the  $2\theta$  range 20–120° using filtered CuK $\alpha$  at a goniometer speed of 0.5° per minute and a chart speed of 20 mm/min. All measurements were made at room temperature. Figure 1: The XRD patterns of CuInSe<sub>2</sub> powders are given in Figure 1. The observed integrated intensities have been corrected for thermal diffuse scattering using the method of Chipman and Paskin [7].

(2) Transmission Electron Microscope (TEM) for microstructural analysis of individual particles.

### 3. Analysis of Data

The procedure for the determination of directional mean-square amplitudes of vibration  $\langle u_{\parallel}^2 \rangle$  and  $\langle u_{\perp}^2 \rangle$  from the intensity data and the estimation of associated errors is as discussed by Gopi Krishna et al [8]. The average mean square amplitude  $\langle u_{av}^2 \rangle$  can be obtained from the relation,

$$\langle u_{av}^2 \rangle = 1/3 (\langle u_{\parallel}^2 \rangle + 2 \langle u_{\perp}^2 \rangle) \quad (1)$$

and the directional Debye-Waller factors  $B_{\perp}$  and  $B_{\parallel}$  were obtained from the equations

$$\frac{B_{\perp} = 8\pi^2 \langle u_{\perp}^2 \rangle}{B = 8\pi^2 \langle u_{av}^2 \rangle} \quad (2)$$

The mean Debye-Waller factor B is given by

$$B = (2B_{\perp} + B_{\parallel}) / 3$$

The directional Debye temperatures  $\theta_{\perp}$ ,  $\theta_{\parallel}$  and mean Debye temperature  $\theta_M$  were obtained from  $B_{\perp}$ ,  $B_{\parallel}$  and B, respectively using the Debye-Waller theory [9] relation,

$$\left\{ \begin{array}{l} \frac{B}{B_{\perp}} = \frac{(6h^2 / M k_B \theta_M) W(X)}{(6h^2 / M k_B \theta_{\perp}) W(X)} \\ \frac{B}{B_{\parallel}} = \frac{(6h^2 / M k_B \theta) W(X)}{(6h^2 / M k_B \theta_{\parallel}) W(X)} \end{array} \right\} \quad (3)$$

Where h is the Planck's constant,  $k_B$  the Boltzmann constant, M the atomic weight. The function W(X) is given by

$$W(X) = [\phi(X)/X + (1/4)] \quad (4)$$

where  $X = \theta_M/T$ , T is the temperature of the crystal and  $\phi(X)$  is the Debye function. The values of W(X) for a wide range of X can be obtained from standard tables [10].

Lattice strain and Particle size determination

When the size of the individual crystals is less than about 100nm the term "particle size" is usually used. When the crystallites of a material are smaller than 100nm, they have too small a number of parallel diffraction planes and so they produce broadened diffraction peaks instead of a sharp peak. Lattice strain present in the sample is another cause of broadening of Bragg diffraction peaks. In addition to this, there are instrumental factors such as unresolved  $\alpha_1$  and  $\alpha_2$  peaks, imperfect focusing which lead to the line broadening. There are various methods in practice to estimate the particle size. X-ray diffraction is a simpler and easier approach for the determination of precise particle size and the lattice strain in powder samples. The principle involved in the X-ray diffraction approach is precise quantification of the broadening of the Bragg diffraction peaks. Scherrer equation, Hall-Williamson method and Warren-Averbach method are some of the techniques based on this principle. Of the above methods, Scherrer equation method for the estimation of particle size does not take into account the broadening due to lattice strain present in the sample. As such in the present investigation, the lattice strains have been estimated using Hall-Williamson method. Recently, Bharati *et al* [16] have used this method to estimate the lattice strain and particle sizes of silver nano particles and composite silver nano particles. In this method the integral breadth of the diffraction

peak is determined. The integral breadth is given by the integrated intensity divided by the maximum intensity. Thus, the observed peak broadening  $B_o$  may be represented as

$$B_o = B_i + B_r \quad (5)$$

where  $B_o$  is the observed peak broadening in radians,  $B_i$  is the instrumental broadening in radians and  $B_r$  is the broadening due to the small particle size and lattice strain. The instrumental broadening has been estimated using a pure strain-free fine sodium chloride powder sample subjected to XRD under identical conditions as those for the strained metallic powders. Eq. (5) holds good if the diffraction peaks exhibit purely Cauchy profile. However, when the diffraction peaks are partly Cauchy and partly Gaussian for profiles, the following relation between  $B_o$ ,  $B_i$  and  $B_r$  holds good, Bharati *et al* [11].

$$B_r = [(B_o - B_i)^2 - B_i^2]^{1/2} \quad (6)$$

Now, according to Scherrer equation, the broadening due to small particle size may be expressed as

$$B_c = \frac{k\lambda}{t} \cos\theta \quad (7)$$

where  $B_c$  is the broadening solely due to small crystallite size, K a constant whose value depends on particle shape and usually taken as unity, t the crystallite size in nanometers,  $\theta$  the Bragg angle and  $\lambda$  is the wavelength of incident X-ray beam in nanometers. Similarly, according to Wilson [12], the broadening due to lattice strain may be expressed by the relation,

$$B_s = \varepsilon \tan\theta \quad (8)$$

where  $B_s$  is the peak broadening due to lattice strain and  $\varepsilon$  the strain distribution within the material and  $\theta$  is the Bragg angle. Based on Eqs. (7) and (8) the total peak broadening  $B_r$  may be expressed as,

$$B_r = \frac{k\lambda}{t \cos\theta} + \varepsilon \tan\theta \quad (9)$$

which can be written as

$$B_r \cos\theta = \frac{k\lambda}{t} + \varepsilon \sin\theta \quad (10)$$

Figure 2: The plot of  $B_r \cos\theta/\lambda$  versus  $\sin\theta/\lambda$  is a straight line with slope equal to  $\varepsilon$  and hence the particle size 't' can be estimated from the intercept. Typical Hall-Williamson plot between  $B_r \cos\theta/\lambda$  and  $\sin\theta/\lambda$  is shown in Figure (2).

The lattice strains were determined from the plot of  $B_r \cos\theta/\lambda$  against  $\sin\theta/\lambda$  following standard procedures [13]. The measured half-widths were corrected for instrumental broadening with reference to a pure strain-free silicon powder. The variation of particle size with milling time is within the limits of experimental errors. This shows that while the milling is enough to create strains, it affect the particle size to a measurable extent. A typical Hall-Williamson plot is shown in Figure 2 for Cd after milling for 20 hours.

## 4. Results and Discussion

Table-1: The values of the particle size, lattice strain, root mean square amplitude of vibrations, Debye-Waller factor and Debye temperature of CuInSe<sub>2</sub> powders, ground for different durations, obtained in the present study are given in Table-1. Although, values of Debye-Waller factor, amplitude of vibration and Debye temperature in the 'a' and 'c' directions have been determined separately, the average values of these quantities are given in Table-1. as the objective of the present work is to investigate the strain dependence of Debye-Waller factors. Debye-Waller factor Mg powder sample carries an effect due to lattice strain. While comparing the Debye-Waller factors calculated from the lattice dynamical models with experimental results Vetelino et al [14] have attributed the difference to inaccuracies in the experimental values caused by neglecting the TDS corrections. The repeated milling of the powder sample leads to lattice distortion which gives rise to microstrains in the lattice. These microstrains increase the contribution of static component of Debye-Waller factor. Thus both lattice strain and the observed Debye-Waller factor, which is the sum of static and thermal components, increase with grinding time. Thus, whenever Debye-Waller factors are determined from X-ray intensities on powder samples, it is desirable, to make an estimate of the lattice strain and if the strain is large, a suitable correction is to be made as in the present study.

Glyde [15] derived the following relation between the energy of vacancy formation ( $E_f$ ) and the Debye temperature ( $\theta$ ) of a solid. The relation is

$$E_f = A (k/h)^2 M \theta^2 a^2 \quad (11)$$

where  $a$  is the interatomic spacing,  $A$  a constant shown to be equal to  $1.17 \times 10^{-2}$ ,  $M$  the molecular weight and  $h$  and  $k$  are the Plank's and the Boltzmann's constants, respectively. Glyde recommended the use of X-ray based values in eq. (11). The validity of eq.(11) was verified for a number of fcc, bcc and hcp metals [16]. Therefore, the X-ray Debye temperatures obtained in the present work have been used to study the variation of vacancy formation energy as a function of lattice strain in Mg. The values of vacancy formation energies are also included in Table-1.

## 5. Conclusion

Cd powder was strained by milling for 25 hours. From a study of X-ray diffractograms recorded at different stages of milling, it is observed that milling for 25 hours has systematic effect on the particle size. However, the milling produces lattice strain and also enhances the effective Debye-Waller factor. The variation of energy of vacancy formation as a function of lattice strain has been studied.

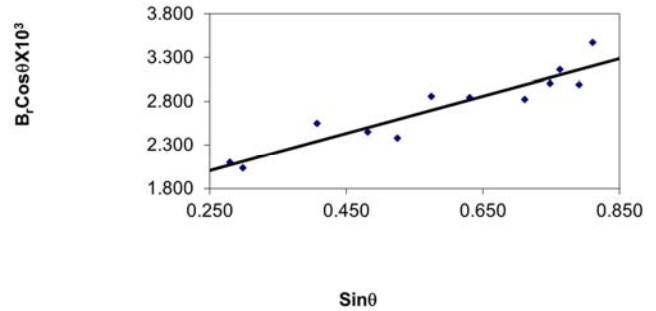


Figure 1. Plot of  $B_r \cos \theta / \lambda$  Vs  $\sin \theta / \lambda$  for Cd after milling for 20 hours.

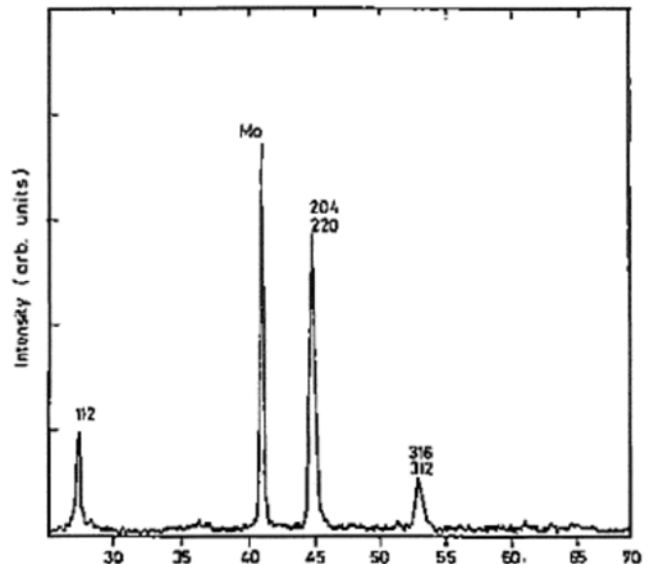
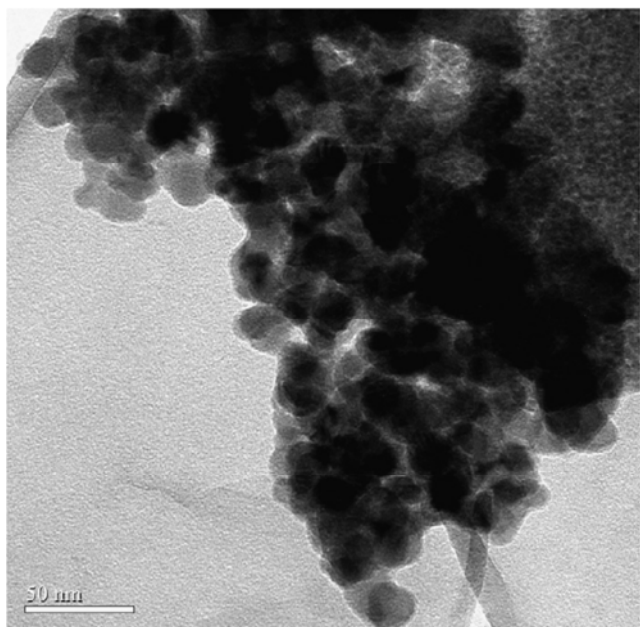


Figure 2. XRD patterns of CuInSe<sub>2</sub>.

**Table 1.** Values of particle size ( $t$ ), lattice strain ( $\epsilon$ ), mean Debye-Waller factor ( $B$ ), root mean square amplitudes of vibration  $\langle u \rangle$ , mean Debye temperature ( $\theta_M$ ) and energy of vacancy formation ( $E_f$ ) of CuInSe<sub>2</sub> nano powder by XRD of the samples prepared by fixing the reaction temperature 200°C and the time varied from 10 to 20 hours.

Material	Time (Hrs)	$\epsilon \times 10^3$	$t$ (nm)	$u$ (Å)	$B$ (Å <sup>2</sup> )	$\theta_M$ (K)	$E_f$ (eV)
CuInSe <sub>2</sub>	10	1.24	51.6	0.00167	0.1321	281	0.47
	12	1.29	46.7	0.00176	0.1388	274	0.43
	14	1.32	37.4	0.00184	0.1456	267	0.35
	16	1.36	32.8	0.00196	0.1544	260	0.36
	18	1.40	29.4	0.00203	0.1599	255	0.32
	20	1.48	25.8	0.00210	0.1662	250	0.28



**Figure 3.** A TEM micrograph of spherical CuInSe<sub>2</sub> particles prepared by using deionized water as washing agent.

## References

- [1] W. U. Huynh, J. J. Dittmer, A. P. Alivisatos, *Science* 295 (2002) 2425–2427.
- [2] B. Sun, E. Marx, N. C. Greenham, *Nano Letters* 3 (7) (2003) 961–963.
- [3] N. Kavcar, *Solar Energy Materials and Solar Cells* 52 (1998) 183.
- [4] H. J. Moller, *Semiconductors for Solar Cells*, Boston, 1993.
- [5] B. Li, Y. Xie, J. Huang, Y. Qian, *Adv. Mater.* 17 (1999) 1456–1459.
- [6] K. B. Tiang, Y. T. Qian, J. H. Zeng, X. G. Yang, *Adv. Mater.* 34 (2003) 448–450.
- [7] D. R. Chipman and A. Paskin, *J. Appl. Phys.* 30, 1938 (1959).
- [8] N. Gopi Krishna, D. B. Sirdeshmukh, B. Rama Rao, B. J. Beandry and K. A. Jr. Gschneidner, *Indian J Pure & Appl Phys.* 24, 324 (1986).
- [9] R. W. James, *The optical principles of the diffraction of x-rays* (Bell and Sons, London, 1967).
- [10] *International tables for X ray crystallography*, Vol. III (Kynoch press, Birmingham) (1968).
- [11] Bharati, R., Rehani, P. B., Joshi, Kirit N., Lad and Arun Pratap, *Indian Journal of Pure and Applied Physics*, 44, (2006) 157-161.
- [12] Wilson, A. J. C., (1949). *X-ray Optics* (Methuen, London).
- [13] Kaelble, E. F., *Handbook of X-rays* (New York Mc Graw Hill) (1967).
- [14] J. F. Vetelino, S. P. Gaur, S. S. Mitra, *Phys. Rev. B* 5, 2360 (1972).
- [15] H. R. Glyde, *J. Phys and Chem Solids* (G. B), 28, 2061 (1967).
- [16] *Micro-and Macro-Properties of Solids*, Springer Series in Material Science, (2006).